ULTRASONIC DETECTION AND CHARACTERIZATION OF MICROSPHERICAL DEFECTS IN MODEL CERAMICS

Arthur Stockman, Patrick Mathieu, and Patrick S. Nicholson

Ceramic Engineering Research Group, McMaster University

Hamilton Ontario, Canada

INTRODUCTION

Ceramic materials can replace metals in many applications requiring high strength and resistance to environmental factors. This can be accomplished only when the ceramic components are sufficiently reliable in service. Modern proof testing methods although capable of separating good components from defective ones, up to the limit of the test, cannot assure that all potentially destructive defects have been found. Long term creep effects and growth of defects due to stress can lead ultimately to failure of a component. Therefore, it is necessary to develop nondestructive testing techniques which can be used in a quality control environment or even at the site of the component. Several techniques are available based on metals evaluation; however, the size of the defects which must be detected in ceramics are in the order of 10 μm so these techniques require development to both detect and characterise defects in ceramics.

The technique presently chosen to examine ceramics was ultrasound. It facilitates the scanning of the component under computer control; and, the use of focussed transducers can yield high sound intensity at the site of a defect and give pin-point spatial resolution. The detection of minute voids and inclusions is most easily performed with high frequency ultrasound (>100 MHz) however immersion scanning in water and grain scattering in ceramics places an upper limit <200 MHz upon useful sound frequencies. Transducers in this frequency range are not commercially available and a program is underway to develop higher frequency transducers. The present study utilised commercial transducers operating at 25 MHz and defects larger than 30 μm. At this frequency, small defects are scatterers rather than reflectors and analysis of the returning ultrasound signals requires some processing to determine the nature of the defect. Through the application of monotone plane wave theory to the sound field at the focus of a pulsed transducer, information about the character of the scattered ultrasound has been obtained.

Finally, the greatest obstacle facing NDE of ceramics is the lack of optically characterisable defects. To overcome this problem, spherical and near spherical oxide particles (diameters <200 μm) were imbedded in glass. The use of glass as a model host matrix facilitates complete optical characterization of the defect and scattering theory can be compared with experiment to reach a better understanding of the processes involved.

THEORY

Scattering of monotone plane wave ultrasound by spherical obstacles having diameters in same order as the wavelength can be described by the theory of Ying and Truell [1] with the correction of Gubernatis [2]. In this theory an incoming plane wave of a single frequency is scattered as longitudinal and shear spherical waves. The terms of interest here are those corresponding to the backscattered longitudinal wave. For a detector far from the scatterer the pressure can be given by:

$$P(k,a) = ka \exp(-ikz_f) \sum_{m=0}^{\infty} (2m+1) A_m \qquad (1)$$

where P(k,a) is the pressure at the transducer, k is the wavenumber of the ultrasound, a is the defect radius, and z_f is the focal length of the transducer. The complex coefficient A_m contains the information for scattering of a single frequency of ultrasound from a spherical defect with the host and defect material parameters of density, and longitudinal and shear velocities. This simple scattering model can applied directly if a continuous plane wave is incident upon the defect.

In the present work a pulsed and focussed transducer was used,and to make the experimental situation and theory compatable, the theory of O'Neil [3] describing the sound field at the focus of a single frequency transducer was expanded into plane waves. This yields:

$$p = p_{max} \exp[i(2\pi ft - k'\Delta z)]/ k' \qquad (2)$$

where:

$$\Delta z = z - z_f$$

and:

$$k' = \frac{k}{2} ([1-(D/2z_f)^2]^{\frac{1}{2}} + 1)$$

Here f is the frequency, p is the pressure along the z axis away from the center of the transducer, h is a function of the transducer radius of curvature, R, and the diameter, D. The maximum pressure p_{max} is also a function of the transducer's dimensions; however, it will remain fairly constant over a distance of 400 μm from the focus of the transducer in all directions [4]. This distance is sufficient to cover the volume included by the defect.

Finally, to account for the frequencies introduced into the sound field by pulsing the transducer and the receiver response, the technique employed of Tittman et al [5] for a planar transducer has be used. The frequency response of the system is obtained by Fourier transforming a signal reflected from a flat surface in the far field of a planar transducer. In the case of a focussed transducer the plane of the surface must correspond to the focal plane of the transducer. This data is then convolved with the single frequency backscattered response of the defect to yield a net response. In order to simplify the calculations, the frequency spectrum of the surface reflection is approximated by a Gaussian distribution with a center frequency, f_c, - also known as the frequency at maximum amplitude (FMA) - and a width defined at the half maximum amplitude points (FWHM), f_{FWHM}. In the calculations the maximum amplitude is normalized so that the effects of attenuation can be disregarded. The total pressure response at the transducer, P_r, is given by:

$$P_r = \exp(-4 \ln 2 [(f-f_c)/f_{FWHM}]^2) ka \sum_{m=0}^{\infty} (2m + 1) A_m \qquad (3)$$

The resulting complex frequency spectra can be Fourier transformed to yield the time signals and the magnitude frequency spectrum can be obtained by taking the modulus.

EXPERIMENT

In order to obtain samples which can be used for scanning and signal analysis and which can be optically characterised without destroying the sample, glasses were prepared into which spherical or near spherical oxide inclusions were imbedded. The glass compositions were determined so as to match the thermal expansion properties of the zirconia and magnesia particles. This was necessary to yield intimate contact between the host glass and the defect. The inclusions were prepared using a multiple rolling mill process then sorted to obtain the most spherical specimens. These were stirred into the molten glass which was then solidified and annealed. The voids used in this study were produced in the manufacturing process. Samples were scanned ultrasonically to locate the defects.

The scanning system used can be divided into three parts: ultrasonics, data acquisition and the scanner. Figure 1 shows these components in a block diagram form. The ultrasonic part of the system consists of a commercial focussed 25 MHz transducer excited by a voltage spike from a pulser - receiver. This unit was operated in the pulse-echo mode. The part of the signal following the top surface reflection was selectively gated to a video detector, the output of which was proportional to the amplitude of the incoming signal. This video detected signal was routed to the data acquisition system. The acquisition system consists of a minicomputer and a high speed programmable digitiser. One channel of the digitiser is connected to the video output (indicated as 'peak detector' in Fig. 1) while the other channel is connected to the radio frequency (r.f.) output of the receiver (indicated as 'digitizer' in Fig. 1). The minicomputer can record signals from either channel on magnetic media for future analysis or while scanning it can seek peaks in the video signal. The minicomputer also controls the mechanical scanning of samples by providing the the signals to the X-Y scan controller. The scan controller is a part of the scanner which has stepper motors on the X and Y axes and a manual Z-axis to adjust the height to the transducer above the sample. Signals from the scan controller yield an X axis resolution of 0.02 mm and a Y axis resolution of 0.01 mm. The computer keeps track of the motion of these axes and the amplitude of the video signal so that the backscattered signal amplitudes from defects can be correlated with their position. In this way outlines of the defects can be obtained. However, scattering from the defects which have dimensions in the order of the wavelength of the sound, tend to be

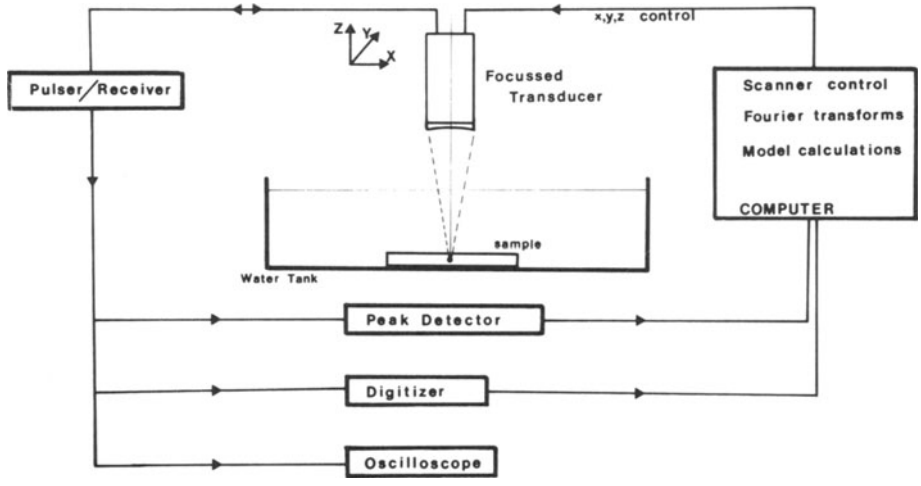

Figure 1 Scanning system for experiment.

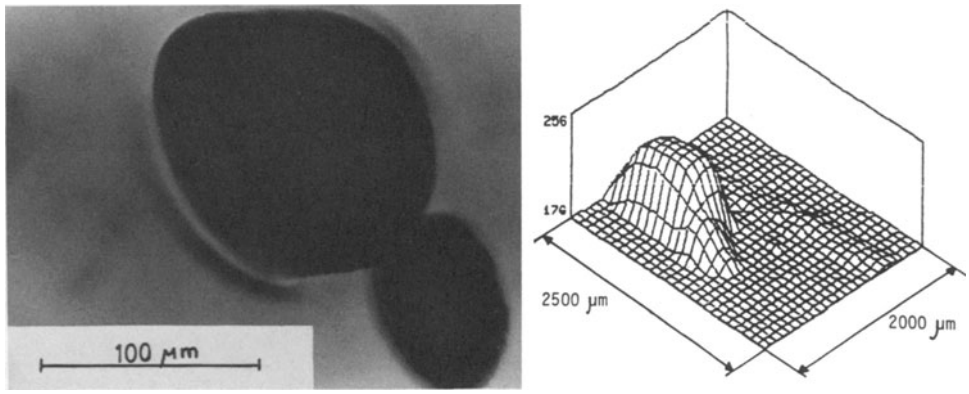

Figure 2 Photograph of two closely spaced defects and the resulting carpet diagram from the scan of the sample.

non-directive so that defects appear larger in the figures than the really are. Figure 2 is an example of a scan of two closely spaced inclusions shown in the photograph. Scattering gives the appearance of one defect; but the relative separation and irregular shape are indicated. It is this discrepancy between actual and observed size that prompts the need for signal analysis.

RESULTS AND DISCUSSION

After scanning, the transducer can be returned to the position of the defect and the digitised waveforms recorded. These rf signals can subsequently be Fourier transformed to yield their frequency spectra. Examples of time signals and their corresponding magnitude frequency spectra are shown in Fig. 3 for zirconia inclusions of various sizes. The time and frequency spectra calculated from theory and presented in Fig. 4 for spherical zirconia inclusions. Comparison of figures 3 and 4 shows that similarities exist between the theoretical and experimental waveforms but quantitative comparisons would be difficult in the time domain. In the frequency domain the FMA and the FWHM are easily measured. Since these correspond to the input Gaussian distribution parameters of center frequency and FWHM it is also possible to examine the effect the scatterer has had upon the incoming signal. Figure 5 is a comparison of theoretical variations (solid lines) and experimental data (solid dots) of FMA and FWHM versus defect diameter. The open circles indicate signals acquired from a magnesia inclusion which was poorly bonded to the glass.

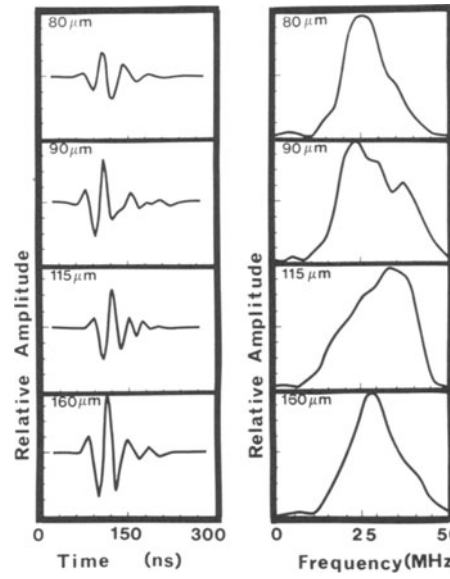

Figure 3 Waveforms and magnitude spectra for backscattered signals from zirconia inclusions in a glass matrix.

The shapes of these curves can by explained by resonances of the defect with particular wavelengths present in the incoming pulse. These resonances are manifest as 'creeping' or Franz waves which circumnavigate the defect [6]. In the waveforms of Figures 3 and 4 these waves appear as a smaller tailing wave after the main wave, depending upon the size of the defect. In the frequency spectra these resonances appear as distortions of the incoming signal spectrum and the nonlinear forms of the FMA and FWHM curves are the result of these resonances appearing at different frequencies for different defects. However, the theory does predict the backscattered signal from spherical defects in the focal zone of a pulsed focussed transducer.

The main drawback to the theory is that the host and defect densities and shear and longitudinal velocities must be known to perform the calculations. Thus some type of iterative process would be necessary to determine what kind of unkown defect is present. In order to investigate which parameters are the most significant in determining the backscattered signal shape, calculations were performed keeping the host material parameters constant. The results of these calculations are presented in Fig. 6 with lines representing scattering from zirconia and magnesia inclusions and voids. The overall shapes of the curve change little for the different types of defects. This means that the major effects upon the resonances are the defect size and the host material parameters. Further calculations were performed for different glass types fixing magnesia as the defect type. These results are shown in Fig. 7. Here the shapes of the curves vary significantly for the two different glasses. In terms of defect characterisation, this result suggests that the iterative process could be started with an average set of defect material parameters and specific host material parameters. Thereafter, the defect parameters would be changed to obtain agreement with experimental data. Finally, given that sufficient

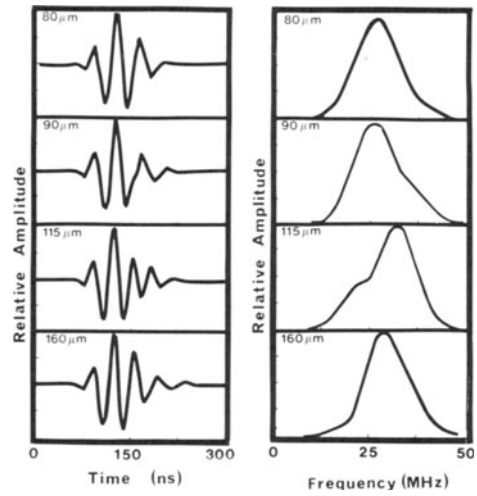

Figure 4 Waveforms and magnitude spectra calculated for spherical inclusions of zirconia in glass. Sizes are indicated in the left-hand corner of each waveform.

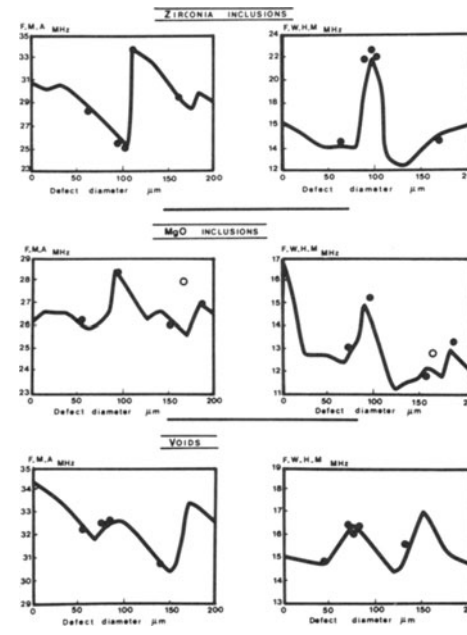

Figure 5 Comparison of experimental (solid dots) and theoretical results (solid lines) for magnitude spectrum parameters of FMA and FWHM versus defect diameter. Open circles represent scattering from poorly bonded defect.

number of similar defect types are present, their size and character may be determined.

CONCLUSIONS

Using a computer controlled scanning system, it is possible to locate defects <100 μm spatially. Defect characterisation can be performed by examining resonances in the frequency response of the defect, and the effects these resonances have upon the magnitude frequency spectrum of the generated ultrasound. For oxide inclusions in glass the resonances are most strongly affected by the glass density, shear and longitudinal sound velocities. Changing these parameters for the inclusion shifts the curve about a mean form; so to determine the density, longitudinal and shear velocities , which determine the chemical nature of the defect, a set of average oxide parameters could be used for initial calculations and appropriate changes made to these average values to obtain a fit to the data.

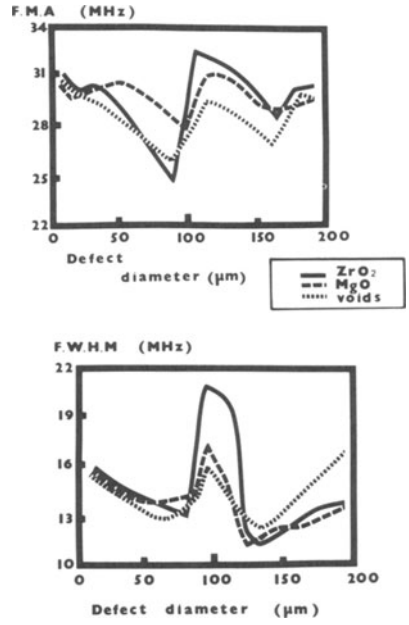

Figure 6 Comparison of theoretical scattering FMA and FWHM curves for different defect types keeping the host glass matrix constant.

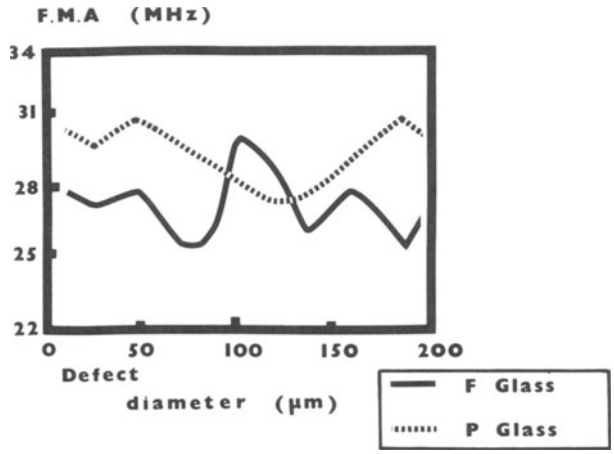

Figure 7 Comparison of theoretical scattering FMA and FWHM curves for different glass types keeping defect type constant.

REFERENCES

1 C. F. Ying and R. Truell, J. Appl. Phys., 27, 1086 (1956).
2 J. E. Gubernatis, E. Domany, J. A. Krumhansl, and M. Huberman, J. Appl. Phys., 48, 2812 (1977).
3 H. T. O'Neil, J. Acoust. Soc. Am, 21, 516 (1949).
4 J. A. Archer-Hall and A. I. Ali-Bashter, NDT International, April 1980, 51.
5 B. R. Tittmann, R. E. Cohen, and J. M. Richardson, J. Acoust. Soc. Am., 63, 68 (1978).
6 G. C. Gaunaurd, E. Tanglis, H. Uberall, and D. Brill, Nouvo Cimento, 76B, 153 (1983).